Fasting protects mice from lethal DNA damage by promoting small intestinal epithelial stem cell survival

Kelsey L. Tinkum[a,b,1], Kristina M. Stemler[c,1], Lynn S. White[a,b], Andrew J. Loza[d], Sabrina Jeter-Jones[c], Basia M. Michalski[a], Catherine Kuzmicki[a], Robert Pless[e], Thaddeus S. Stappenbeck[f], David Piwnica-Worms[a,b,c,g,2], and Helen Piwnica-Worms[a,c,d,2]

[a]Department of Cell Biology and Physiology, Washington University School of Medicine, St. Louis, MO 63110; [b]Mallinckrodt Institute of Radiology, Washington University School of Medicine, St. Louis, MO 63110; [c]Department of Cancer Biology, The University of Texas MD Anderson Cancer Center, Houston, TX 77030; [d]Department of Internal Medicine, Washington University School of Medicine, St. Louis, MO 63110; [e]Department of Computer Science and Engineering, Washington University in St. Louis, St. Louis, MO 63130; [f]Department of Pathology and Immunology, Washington University School of Medicine, St. Louis, MO 63110; and [g]Department of Cancer Systems Imaging, The University of Texas MD Anderson Cancer Center, Houston, TX 77030

Edited by Melanie H. Cobb, University of Texas Southwestern Medical Center, Dallas, TX, and approved November 5, 2015 (received for review May 11, 2015)

Short-term fasting protects mice from lethal doses of chemotherapy through undetermined mechanisms. Herein, we demonstrate that fasting preserves small intestinal (SI) architecture by maintaining SI stem cell viability and SI barrier function following exposure to high-dose etoposide. Nearly all SI stem cells were lost in fed mice, whereas fasting promoted sufficient SI stem cell survival to preserve SI integrity after etoposide treatment. Lineage tracing demonstrated that multiple SI stem cell populations, marked by *Lgr5*, *Bmi1*, or *HopX* expression, contributed to fasting-induced survival. DNA repair and DNA damage response genes were elevated in SI stem/progenitor cells of fasted etoposide-treated mice, which importantly correlated with faster resolution of DNA double-strand breaks and less apoptosis. Thus, fasting preserved SI stem cell viability as well as SI architecture and barrier function suggesting that fasting may reduce host toxicity in patients undergoing dose intensive chemotherapy.

stem cells | DNA damage | chemotherapy | fasting

Cancer patients undergoing chemotherapy experience high rates of morbidity, despite regimens that attempt to balance timing and dose intensity to mitigate off-target effects and dose-limiting toxicities (1–3). Interestingly, fasting has been shown to provide host-protective effects against high-dose chemotherapy-induced toxicity in preclinical and clinical studies. For example, etoposide, which forms a ternary complex with DNA and topoisomerase II causing DNA double-strand breaks (DSBs), is far less toxic if mice are fasted before treatment (4). Fasting has also been shown to protect normal, but not cancer cells, from the toxicity of chemotherapy, thereby extending the lifespan of tumor-bearing mice (4–8).

Because of the rapid rate of epithelial cell proliferation in the small intestine (SI), gastrointestinal (GI) toxicity is one of the most common complications for a variety of chemotherapeutic treatments (9). Therefore, we investigated if fasting was capable of mitigating the GI toxicity normally associated with high-dose chemotherapy. Herein, we demonstrate that mice allowed to feed ad libitum before receiving high-dose chemotherapy showed marked histological changes to SI epithelium before death. These histological changes reflected loss of regenerative capacity as a result of stem cell depletion as well as structural damage from inflammatory cell infiltrates, similar to the SI response to high-dose ionizing radiation (10). In contrast, SI homeostasis was preserved in fasted mice by protection of stem cell viability and prevention of proinflammatory cell infiltrates. These results indicate that fasting mitigates GI side effects associated with chemotherapy by activating pathways that preserve SI stem cell integrity and by maintaining barrier function.

Results

Fasting Protects the SI from Lethal Doses of Etoposide. A previous study showed that mice subjected to short-term fasting are protected from lethal doses of etoposide that otherwise kill fed littermates (4). We confirmed this finding in our facility. B6(Cg)-*Tyr*$^{c\text{-}2J}$/J mice were allowed to feed ad libitum or were fasted for 24 h followed by treatment with etoposide (Fig. 1*A*). In all experiments, food was provided immediately after etoposide treatment. Fed mice died between day 5 and day 6 following etoposide administration, whereas fasted mice survived (Fig. 1*B*). To assess overall health, body weight and food consumption were measured daily (Fig. 1 *C* and *D*). Food consumption and body weight of fed mice consistently and dramatically declined after etoposide treatment. In contrast, body weight declined during the 24-h fast but was fully restored to initial body weight after etoposide treatment and refeeding. Food consumption also slowly declined until reaching a steady-state level by day 12 in mice that were fasted before etoposide treatment. There were also striking differences in the activity level and appearance of fed and fasted mice following chemotherapy. The fed cohort became sedentary and exhibited signs of toxicity, including ruffled fur and hunched back posture. In contrast, the fasted cohort remained active, ate immediately, and exhibited no signs of pain or distress following etoposide treatment. Similar findings were observed when fed and fasted *Lgr5*$^{EGFP::CreERT2}$ (leucine-rich repeat-containing G-protein coupled receptor 5) mice were treated with high-dose etoposide (Fig. S1 *A*–*C*) and survival in the fasted cohort was observed for 140 d postetoposide treatment (Fig. S1 *D* and *E*). Importantly, etoposide cleared from the plasma of fed and fasted mice at equivalent rates (Fig. S1*F*).

Significance

Cancer patients undergoing chemotherapy experience high rates of dose-limiting morbidity. Recently, short-term fasting prior to chemotherapy was shown to decrease toxicity. Herein we report that fasting protects multiple small intestinal stem cell populations marked by *Lgr5*, *Bmi1*, or *HopX* expression and maintains barrier function to preserve small intestinal architecture from lethal DNA damage. Our findings provide insight into how fasting protects the host from toxicity associated with high-dose chemotherapy.

Author contributions: K.L.T., K.M.S., D.P.-W., and H.P.-W. designed research; K.L.T., K.M.S., L.S.W., S.J.-J., B.M.M., and C.K. performed research; A.J.L., R.P., and T.S.S. contributed new reagents/analytic tools; K.L.T., K.M.S., and A.J.L. analyzed data; and K.L.T., K.M.S., D.P.-W., and H.P.-W. wrote the paper.

The authors declare no conflict of interest.

This article is a PNAS Direct Submission.

Data deposition: The data reported in this paper have been deposited in the Gene Expression Omnibus (GEO) database, www.ncbi.nlm.nih.gov/geo (accession nos. GSM1855710–GSM1855717).

[1]K.L.T. and K.M.S. contributed equally to this work.

[2]To whom correspondence may be addressed. Email: dpiwnica-worms@mdanderson.org or hpiwnica-worms@mdanderson.org.

This article contains supporting information online at www.pnas.org/lookup/suppl/doi:10.1073/pnas.1509249112/-/DCSupplemental.

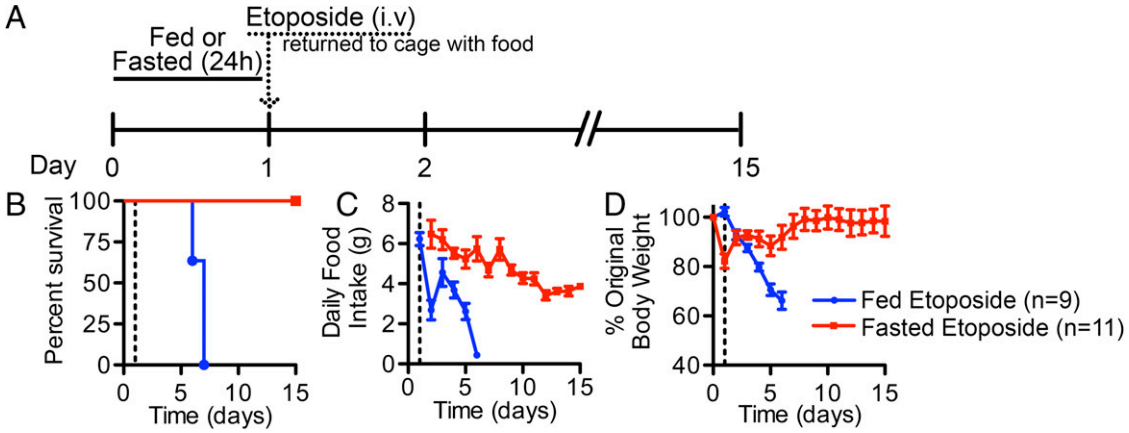

Fig. 1. Effects of high-dose etoposide on integrity of SI in fed and fasted mice. Male and female wild-type mice (4–6 wk of age) were allowed to feed ad libitum or were fasted for 24 h. Etoposide (100 mg/kg) was administered by tail vein injection (day 1). Mice were returned to single-housed cages and access to food was restored immediately after treatment. (*A*) Overall schema and timeline are illustrated. (*B*) Survival was monitored daily for 2 wk up to day 15. (*C*) Food consumption was monitored daily beginning with the 24-h period before etoposide treatment for fed mice and the 24-h period postetoposide treatment for fasted mice. (*D*) Individual mouse body weights were measured daily and were normalized to starting weight. All error bars are ±SEM.

Further examination revealed that the SI mucosa of fed mice exposed to high-dose etoposide displayed significant atrophy 4 d following etoposide treatment (Fig. 2 *A* and *B*), including significant villus shortening, crypt drop out, diminished number of epithelial cells per crypt, and overall shortening of SI length (Fig. 2 *C–E* and Fig. S2 *A* and *B*). In contrast, etoposide-treated fasted animals showed SI hypertrophic crypts throughout the duodenum, jejunum, and ileum (Fig. 2*E* and Fig. S2 *B–D*) compared

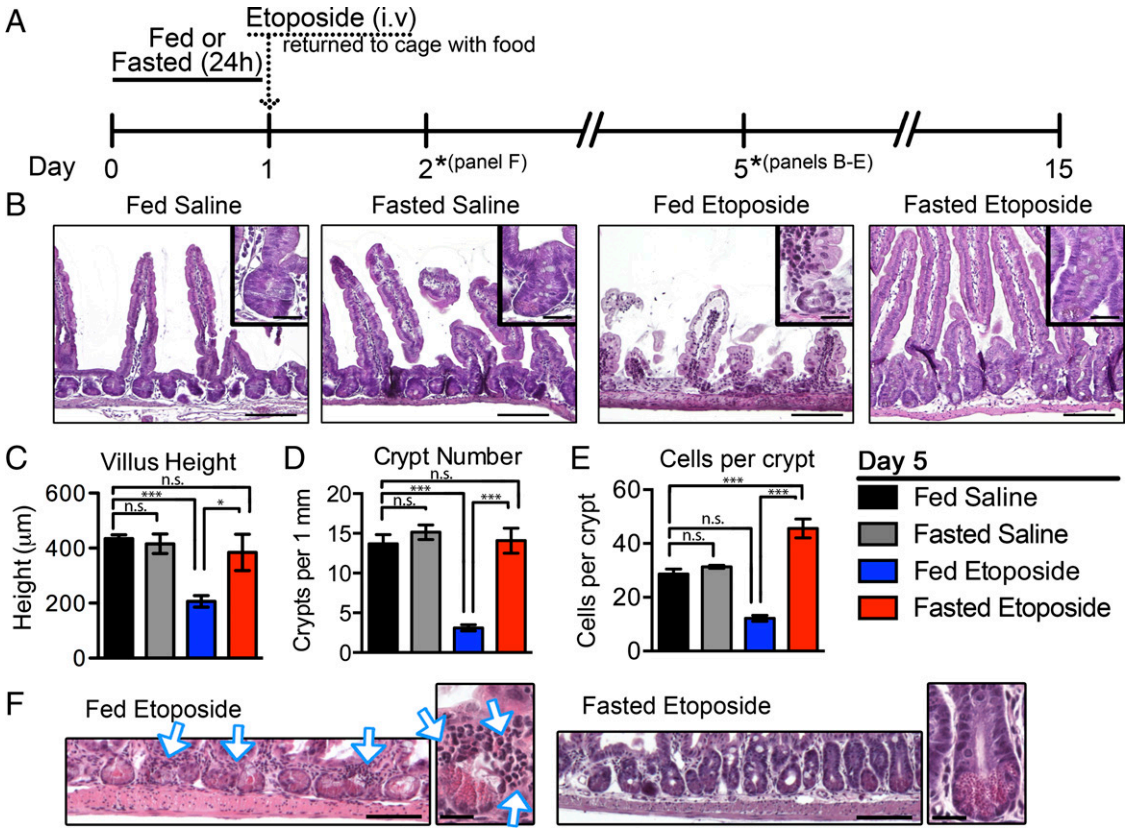

Fig. 2. Fasting preserves SI architecture in the presence of high-dose etoposide. (*A*) Wild-type mice were treated as shown. Asterisks indicate day of killing for experiments in indicated panels. Mice were randomly assigned to four treatment groups ($n = 6–7$ mice per group). (*B*) Representative images of H&E-stained jejunum (day 5). (Scale bars, 200 μm.) Representative crypts shown in *Insets*. (Scale bars, 25 μm.) (*C*) Villi heights ($n = 30$ per mouse) were measured and average value per mouse plotted. (*D*) Number of crypts per length (~20 mm) of SI was quantified for each day 5 sample and average number of crypts per millimeter of SI length plotted. (*E*) Number of cells per crypt was determined ($n = 45$ crypts per mouse) and average number of cells per crypt plotted. n.s., nonsignificant; $*P < 0.05$; $***P < 0.005$ by Tukey posttest of a one-way ANOVA. Error bars are ±SEM. (*F*) *Lgr5*$^{EGFP\text{-}IRES\text{-}CreER/+}$ mice were treated as in *A*. Representative images of H&E-stained jejunum are shown. Arrows indicate neutrophils. [Scale bars, 100 μm (*Left*) and 25 μm (*Right*).]

with their saline-treated fed counterparts. The hypertrophy observed in SI crypts resolved by 10 d postetoposide treatment (Fig. S2 *E* and *F*). Crypt number and villus height were similar in the two fasted experimental groups (Fig. 2 *C* and *D*). In contrast to the SI, the overall length and crypt depth of the colonic mucosa was preserved in etoposide-treated mice regardless of the feeding regimen (Fig. S3). Examination of all other organs showed no obvious gross or microscopic abnormalities in fed or fasted cohorts. Therefore, fasting before etoposide treatment protected mice from etoposide-induced SI damage.

Chemotactic signaling is commonly observed in response to DNA damage (11–13). We previously reported a loss of villus goblet cells and an increase in acute inflammatory cells in the SI of irinotecan-treated mice (14). To determine if fasting before chemotherapy protected against this proinflammatory response, fed and fasted mice (*Lgr5* reporter strain) were treated with 80 mg/kg etoposide (Fig. S4 *A* and *B*) and SI were isolated at various times for analysis. Strikingly, by 48-h postetoposide treatment, large numbers of neutrophils were clustered at the crypt–villus border in the SI of fed mice, which correlated with a complete separation of many crypts from their corresponding villi (Fig. 2*F*). Neutrophils were not observed to infiltrate into the SI of fasted mice following etoposide treatment.

Crypt Stem Cells Maintain Integrity of the SI in Fasted Mice Following Etoposide Treatment. The SI epithelial phenotypes observed in fed versus fasted mice following etoposide treatment suggested that fasting might protect SI stem cells from the lethal effects of high-dose chemotherapy. Populations of SI epithelial stem cells are located in the crypt base intermingled with Paneth cells and in a zone immediately adjacent to Paneth cells in the crypt (15–18). One or both of these stem cell populations potentially provided the source of recovery after damage to the epithelial lining from etoposide. Therefore, stem cell reporter mice for both stem cell populations were used to test which populations were responsible for maintaining SI architecture and function following exposure of fasted mice to high-dose etoposide. We used knockin mice carrying tamoxifen-inducible Cre under the transcriptional control of the mouse *Lgr5* promoter to mark crypt base columnar (CBC) stem cells or the mouse *Bmi1* (B lymphoma Mo-MLV-insertion region 1 homolog) or *HopX* (homeobox-only protein X) promoters to mark stem cells residing in the supra-Paneth (+4) cell pool. These knockin mice were bred to mice carrying the Cre-activatable, floxed-stop *Rosa26-lacZ reporter* (R26R) to induce permanent LacZ (bacterial-β-galactosidase reporter gene) expression, mark $Lgr5^+$, $Bmi1^+$, or $HopX^+$ cells, and enable lineage tracing. Before tamoxifen injection to activate the CreERT2 fusion enzyme, mice were treated with various doses of etoposide to determine the optimal dose that enabled fasted, but not fed mice to survive (Fig. S4 *C*–*H*).

Fed and fasted reporter mice were injected with etoposide followed by tamoxifen 1 and 3 h later (Fig. S5*A*). SI isolated 4 d postetoposide-administration were stained for LacZ expression (Fig. 3 *A* and *B*). Data were quantified using a MatLab imaging program that was designed to enumerate fully-traced crypts in whole-mount sections (Fig. 3*C* and Figs. S6 and S7), enabling ∼1,200 crypts in each image to be counted, totaling a minimum of 3,600 crypts per mouse. The number of fully traced crypts was then normalized to the average number of crypts per length of SI within each strain (Fig. S5 *B* and *C*) to control for strain-dependent crypt dropout.

It was important to determine the average number of crypts per length of SI for each individual stem cell reporter strain under each experimental treatment condition, because *Lgr5* reporter mice were more sensitive to the DNA damaging agent and had to be treated with a slightly lower dose of etoposide (80 mg/kg) compared with *Bmi1* and *HopX* reporter strains (100 mg/kg) to phenocopy overall survival curves between fed and fasted mice (Fig. S4). Thus, in *Lgr5* reporter mice, there are more crypts per millimeter of SI under the fed etoposide treatment condition compared with *Bmi1* or *HopX* reporter mice (Fig. S5*C*). As seen in Fig. 3*C*, fasting afforded significant protection of crypt stem cells marked by *Bmi1* or *HopX* expression from high-dose etoposide. There was a strong trend toward fasting-induced protection of CBC stem cells as well, although this did not reach statistical significance ($P = 0.069$). This statistical difference between +4 stem cells and CBC stem cells may be because of the higher number of crypts preserved under fed etoposide treatment conditions in *Lgr* reporter mice as a result of the lower dosing of these mice. Nonetheless, a direct comparison of the normalized traced crypts in fasted etoposide-treated mice demonstrated no significant difference between any of the strains (Fig. S5*D*). Furthermore, each of the three stem cells marked by *Lgr5*, *Bmi1*, or *HopX* expression were capable of giving rise to an entire crypt within 4 d postetoposide treatment (Fig. 3 *A* and *B*), and an entire crypt-villus unit within 8 d (Fig. S5*E*), indicating that each stem cell population is sufficient to repopulate SI epithelium in fasted mice following exposure to high-dose etoposide.

Fasting Preserves SI Stem Cells in Etoposide-Treated Animals. To confirm fasting-mediated protection of SI stem cells in the absence of tamoxifen-mediated lineage tracing, we monitored the viability of SI stem cells in fed and fasted mice following etoposide treatment by establishing cultures of fast-cycling, $Lgr5^+$ stem cell-enriched epithelial spheroids from treated mice (19, 20). The culture conditions used conditioned medium containing Wnt3a, R-spondin 3, and Noggin to support the growth of mouse intestinal epithelial spheroids that are enriched for stem cells (20–22). Under these culture conditions, stem cells do not differentiate into the organoid/bud-like structures seen using protocols published by others (23). Significantly more stem cell-enriched epithelial spheroids were generated from SI crypts isolated from mice that had been fasted before etoposide-treatment compared with their fed counterparts (Fig. 3 *D* and *E*). Importantly, these spheroids could be successfully passaged in culture (Fig. 3*E*). Significantly more spheroids were obtained from all saline-treated animals relative to all etoposide-treated animals, demonstrating that, although many stem cells were killed by high doses of etoposide, fasting protected a subset of stem cells that were able to proliferate and maintain SI structure and function.

Resolution of DNA DSBs in SI Stem Cells in Fasted vs. Fed Mice. We next analyzed the time course of SI stem cell responses to high-dose chemotherapy in fed and fasted animals, specifically focusing on $Lgr5^+$ stem cells using $Lgr5^{EGFP::CreERT2}$ mice. Overall survival and tissue responses of fed and 24-h fasted $Lgr5^{EGFP::CreERT2}$ knockin mice to high-dose etoposide were similar to that of fed and fasted wild-type mice and other reporter mice (Fig. S4). As seen in Fig. 4*A*, the number of GFP^+ (green fluorescence protein) ($Lgr5^+$) stem cells in the SI crypts of fed and fasted knockin mice were similar up to 3 h postetoposide treatment.

We then assessed DNA replication in GFP^+ ($Lgr5^+$) cells by measuring BrdU incorporation in $Lgr5^{EGFP::CreERT2}$ mice at various times before and after etoposide treatment. As seen in Fig. 4*B* before drug treatment, significantly more BrdU incorporation was measured in the GFP^+ ($Lgr5^+$) cells from fed versus fasted mice, indicating that stem cells responded to fasting by reducing proliferation. In contrast, as seen in Fig. 4*B* at both time points postetoposide treatment, BrdU incorporation was similar in both fed and fasted mice.

To identify pathways that were altered in response to etoposide treatment in fed versus fasted mice, microarray analysis was performed on mRNAs isolated by laser microdissection of the lower third of SI crypts. This area is enriched for stem cells and terminally differentiated Paneth cells. We compared gene expression in these crypt base cells from fed versus fasted mice 3 h postetoposide treatment. Not surprisingly, the top enriched Gene

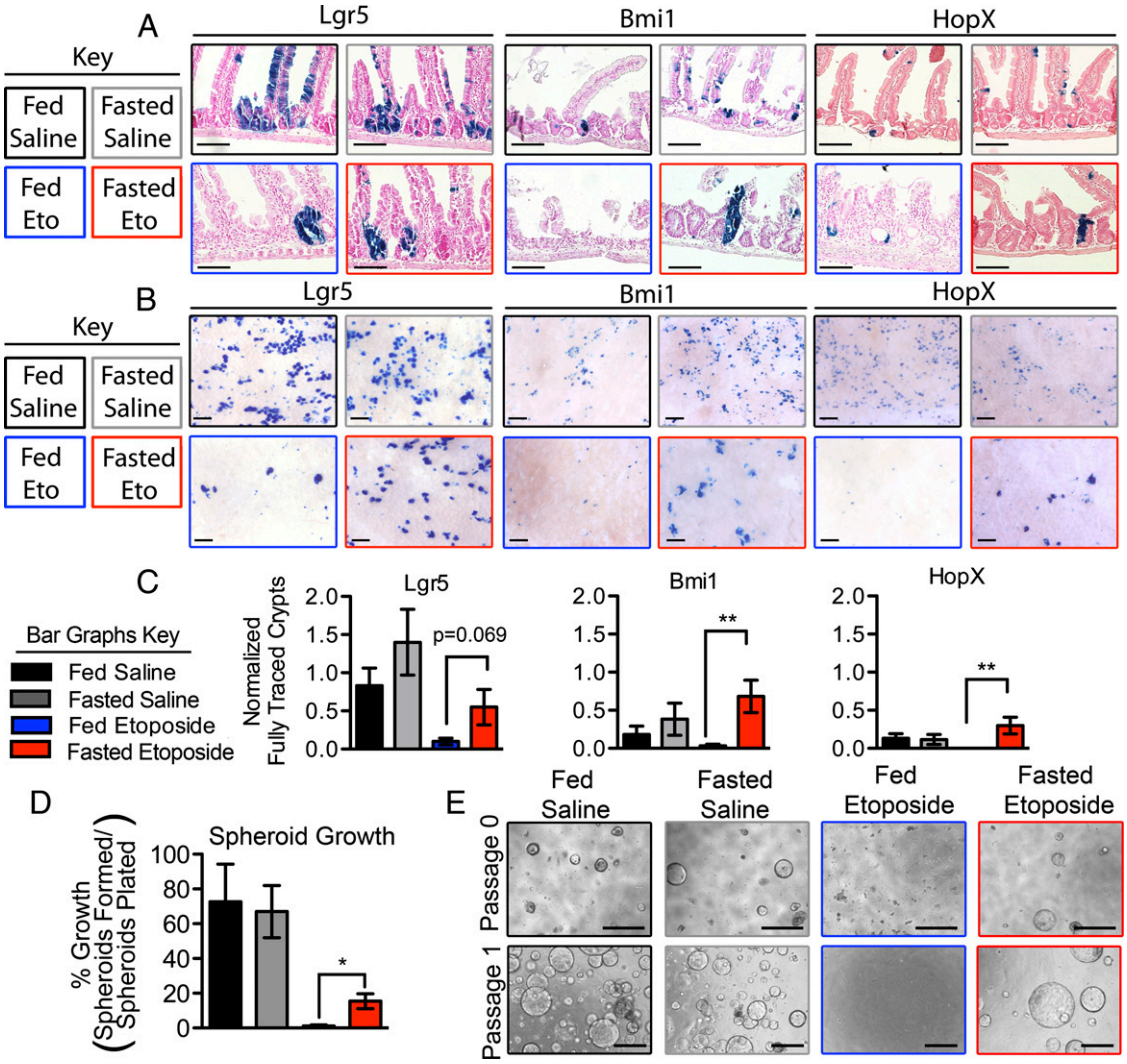

Fig. 3. Fasting protects SI stem cells from high-dose etoposide in vivo and ex vivo. Reporter mice were randomly assigned to four treatment groups and were administered two doses of tamoxifen (t) 1 and 3 h after etoposide. Mice were killed 4 d later (day 5) and SI were harvested and whole-mount tissue stained for LacZ expression (n = 5–6 mice per group). (*A*) Representative images of nuclear fast red-counterstained cross-sections of LacZ-stained jejunums. (Scale bars, 100 μm.) (*B*) Villi were removed from a 2-cm section of LacZ-stained whole-mount tissue for counting traced crypts. Representative images are shown. (Scale bars, 100 μm.) (*C*) The number of fully traced crypts per field of view in whole-mount images was quantified using a custom image analysis program for each day 5 sample and then was normalized to the average number of crypts per millimeter within each strain per treatment. $^{**}P < 0.01$ by one-tailed, Student's t test of normalized arcsine transformed data. (*D*) *Bmi1*$^{CreERI+}$;*R26R* mice were randomly assigned to four treatment groups (n = 3 mice per group). SI crypts were isolated and plated in Matrigel with 50% L-WRN–conditioned media to generate cultures of stem cell-enriched epithelial spheroids. Spheroids were counted after 2 d of culturing in vitro. Spheroid number was normalized to number of crypts originally plated. $^{*}P < 0.05$ by two-tailed, Student's t test. (*E*) Representative images of spheroids after 2 d in culture are shown (*Upper*) at passage 0. Cultures were trypsinized on day 3 and subcultured in fresh Matrigel. Representative images of passage 1 spheroid cultures (2 d posttrypsinization) are shown (*Lower*). (Scale bars, 250 μm.) All error bars are ±SEM.

Ontology functional categories identified as differentially regulated were those related to metabolism (Dataset S1). In addition, cellular response to stress, DNA repair, and DNA damage-response genes were also identified in fasted mice (Dataset S2). This finding suggested that DNA repair capacity might be enhanced in the SI stem cells of fasted mice. To test this, levels of DNA DSBs in Lgr5^{+} stem cells of fed and fasted animals were assessed by costaining sections of SI with antibodies specific for γH2AX (gamma H2A histone family, member X) and GFP. γH2AX staining was similar in all GFP^{+} cells 1.5 h postetoposide treatment (Fig. 4 *C* and *D*). However, by 3 h, γH2AX staining was significantly less in the GFP^{+} cells from fasted animals compared with fed animals (Fig. 4 *C* and *E*). This result indicated that etoposide was bioavailable in the SI of both fed and fasted mice, but resolution of DNA DSBs was more efficient in animals that had fasted before etoposide exposure. Despite an equivalent number of GFP^{+} cells at 3 h postetoposide treatment, there were significantly more GFP^{+} cells that also stained positive for cleaved caspase 3 in the SI crypts of fed versus fasted mice 3 h postetoposide treatment (Fig. 4 *F* and *G*). In contrast, there was no significant difference in the number of transient amplifying (TA) cells undergoing apoptosis between fed and fasted etoposide-treated mice (Fig. 4*H*). These data indicated that fasting selectively protected SI stem cells from high-dose etoposide, in part, by enhancing DNA repair capacity and by reducing apoptosis.

Discussion

GI toxicity is one of the most common complications for a variety of chemotherapeutic treatments (9). At high doses, chemotherapeutic agents destroy SI architecture and compromise

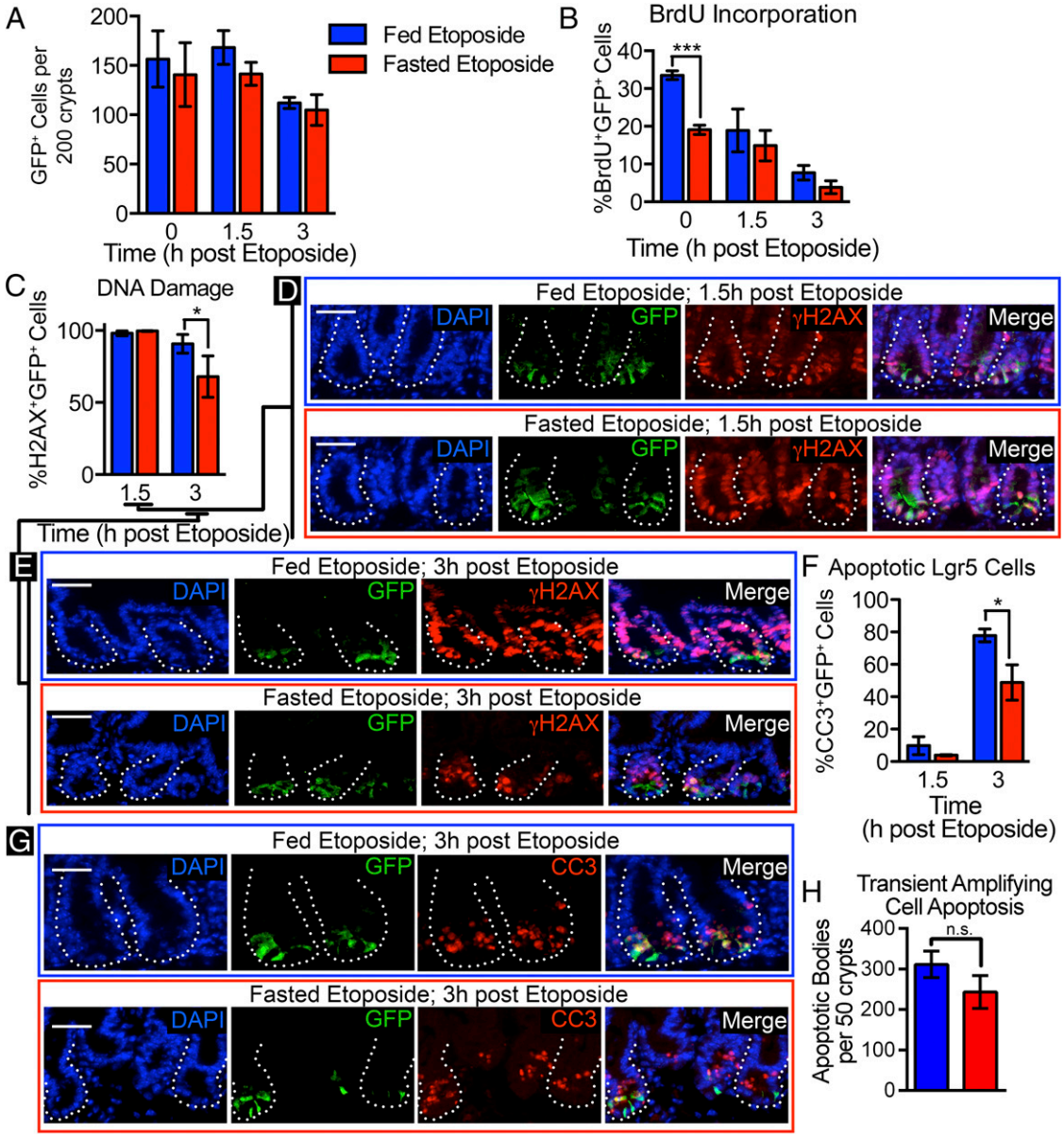

Fig. 4. Fasting alters early response of Lgr5$^+$ stem cells to etoposide. *Lgr5$^{EGFP\text{-}IRES\text{-}CreERT/+}$* mice were randomly assigned to four treatment groups. Two-hundred crypts were evaluated per mouse ($n = 4$ mice per group). Crypts in which the base made direct contact with the lamina propria were analyzed and only GFP$^+$ cells residing at the crypt base were counted. (*A*) The number of GFP$^+$ cells per 200 crypts per mouse at the indicated time points is shown. (*B*) The percentage of cells that costained for GFP and BrdU is shown. BrdU was allowed to incorporate for 1 h before harvest. ***$P < 0.001$ by two-tailed, Student's *t* test. (*C–E*) Percentage of cells that costained for GFP and γH2AX (*C*) and representative images, shown in *D* and *E*. *$P < 0.05$ by two-tailed, Student's *t* test of arcsine-transformed data. (*F* and *G*) Percentage of cells costaining for GFP and cleaved caspase 3 (CC3) is shown (*F*) and representative images from the 3-h time point (*G*). *$P < 0.05$ by two-tailed, Student's *t* test of arcsine transformed data. All error bars are ±SEM. (*H*) Number of apoptotic bodies in the transient amplifying cell zone per 50 crypts at 3-h postetoposide treatment. n.s. is nonsignificant by two-tailed, Student's *t* test. All error bars are ±SEM.

absorptive and barrier functions. Remarkably, we demonstrated that fasting preserves SI structure and function, thereby enabling mice to survive lethal doses of etoposide. Multiple stem cell populations marked by *Lgr5*, *Bmi1*, or *HopX* contributed to maintaining SI homeostasis in response to lethal doses of etoposide. Mechanistic studies demonstrated the following main differences between the SI of etoposide-treated fed and fasted animals: (*i*) DNA repair genes were activated in stem cell-enriched compartments of the SI of fasted animals; (*ii*) DNA DSBs were more quickly resolved in Lgr5$^+$ stem cells of fasted animals; (*iii*) fewer Lgr5$^+$ stem cells underwent apoptosis in fasted animals; and (*iv*) inflammatory cells infiltrated the SI of fed but not fasted animals, thereby inducing collateral damage. Thus, fasting increased DNA repair capacity of SI stem cells and decreased their apoptosis. In addition to protection of SI stem cells, fasting also protected the SI from collateral damage because of neutrophil infiltration, thereby maintaining barrier function. Taken together, these mechanisms explain, in part, how fasting maintains SI homeostasis in the face of lethal DNA damage.

Our data demonstrate that protection of SI stem cells is a key safeguard induced by fasting that insulates mice from the lethal effects of high-dose chemotherapy. Two stem cell populations, classified by their location within the crypt, function to maintain the SI (24). These include the Lgr5$^+$/CBC stem cells located at the crypt base and +4/Bmi1$^+$/HopX$^+$ stem cells, located around

the +4 position from the crypt base (15, 25–27). There is controversy as to the individual contributions made by each of these stem cell niches to maintaining homeostasis under steady-state conditions and restoring homeostasis after a damaging event (16–18, 24). There is also a high level of interconversion among stem cell populations during damaged-induced regeneration of the SI (27, 28). We demonstrated that fasting protects a subset of both CBC and +4 stem cells and that both contribute to SI epithelial renewal after exposure to high-dose etoposide.

In contrast to SI stem cells, fasting did not protect TA cells from high-dose etoposide. Hua et al. (29) demonstrated that $Lgr5^+$ stem cells are more radio-resistant than TA cells because they repair DNA DSBs by homologous recombination much more efficiently. $Lgr5^+$ stem cells and TA cells also use non-homologous end joining to repair DNA DSBs. Thus, adult stem cells may be prewired to be highly proficient at DNA repair in response to genotoxic stress to protect the integrity of their genome and maximize their survival. In our study, enhanced expression of DNA damage repair genes in the SI stem cells of fasted mice relative to their fed counterparts suggests that fasting may further prime SI stem cells (which are already equipped to respond to DNA DSBs) to respond to stress, in this case DNA damage caused by etoposide.

BrdU incorporation was significantly reduced in $Lgr5^+$ stem cells following a 24-h fast, demonstrating that fasting reduced proliferation of these stem cells. This reduction of proliferation might be expected per se to reduce the toxicity of etoposide in fasted mice. However, fasted mice were refed immediately after etoposide injection and $Lgr5^+$ stem cells re-entered the cell cycle upon refeeding (BrdU incorporation was restored). This process rendered stem cells sensitive to the DNA damaging effects of etoposide (DNA DSBs were observed in 99% of $Lgr5^+$ cells). Although there was an equivalent amount of DNA damage in $Lgr5^+$ stem cells from fed and fasted mice at 1.5 h postetoposide treatment, $Lgr5^+$ cells from prefasted mice displayed an enhanced DNA damage response as evidenced by increased expression of DNA repair genes, faster resolution of DNA DSBs, and decreased apoptosis.

The top enriched Gene Ontology functional categories identified as differentially regulated in fed versus fasted etoposide-treated mice were those related to metabolism. Many of the chromatin-modifying enzymes involved in DNA repair depend on metabolic intermediates as cofactors for their activity, thereby directly linking changes in cellular metabolism with DNA repair (30). Interestingly, high levels of NAD^+ (nicotinamide adenine dinucleotide) correlate with radioprotection of human glioma cells (31). Alterations in NAD^+ levels modulate DNA repair and NAD^+ is elevated under conditions of nutrient deprivation. NAD^+-dependent P enzymes [poly(ADP-ribose) polymerase (PARP)1 and PARP2] are immediately activated in response to DNA DSBs and function to regulate both nonhomologous end joining and homologous recombination (30). In our study, *PARP1* gene expression was shown to be elevated in fasted etoposide-treated mice compared with their fed counterparts (Dataset S2). These studies suggest that changes in metabolism converge on the DNA damage-response pathway to repair DNA damage and maintain genomic stability. We have demonstrated that one consequence of the metabolic changes (Dataset S1) associated with fasting followed by etoposide treatment is to induce the DNA damage-response pathway (Dataset S2) in SI stem cells and this correlated with improved kinetics of DNA DSB repair (Fig. 4 *C*–*E*) with a concomitant decrease in apoptosis in these cells (Fig. 4 *F* and *G*), implicating a similar integration of metabolism and DNA damage repair in our study.

Fasting has been shown to protect the host (mice) but not tumors to high-dose chemotherapy (4, 5). Interestingly, fasting on its own suppresses tumor growth in mice, but the greatest therapeutic response is found when fasting is combined with chemotherapy (5). Thus, fasting is capable of sensitizing some tumors to chemotherapy. The growth of some tumors is not reduced by dietary restriction and it has not yet been determined whether tumors that are resistant to dietary restriction are more or less sensitive to chemotherapy (32). One clinical study monitored cancer patients who fasted before receiving chemotherapy (33). Those patients reported fewer side effects (including reduced GI side effects) and where cancer progression was followed there was no evidence that fasting protected tumors or interfered with chemotherapy efficacy. Although fasting can reduce side effects associated with chemotherapy without negatively impacting tumor cell killing, fasting is not feasible for all patients, especially the elderly (34) or those exhibiting cachexia. Future work to delineate a complete mechanistic understanding of how fasting protects SI stem cells may uncover metabolites or other mechanisms that afford patient protection from the side effects of chemotherapy without the need to fast.

Materials and Methods

This study was carried out in accordance with the recommendations in the *Guide for the Care and Use of Laboratory Animals* of the National Institutes of Health (35). The Committee on the Ethics of Animal Experiments at Washington University and the MD Anderson Institutional Animal Care and Use Committee approved all animal protocols used in this study.

Mouse Husbandry. Male and female mice used in this study were 4–6 wk of age. Unless using reporter mice, all experiments were performed using B6(Cg)-*Tyr*$^{c-2J}$/J; (JAX no. 000058). The following mice were also purchased from The Jackson Laboratory: *Bmi1*$^{CreERT/+}$ (stock no. 010531) (15), *Lgr5*$^{EGFP\text{-}IRES\text{-}CreERT2/+}$ (stock no. 008875) (26), *Rosa26*$^{R/+}$ (stock no. 003474) (36), and *C57BL6/J* (stock no. 000664). *HopX*$^{CreERT/+}$ mice were provided by Jonathan Epstein, University of Pennsylvania, Philadelphia (27). LacZ tracings were carried out using mice that were heterozygous for *cre* and *lacZ*. Immunofluorescence experiments were carried out using mice that were heterozygous for *GFP*. Experimental mice were singly housed on aspen bedding. *Bmi1*$^{CreERT/+}$;*Rosa26*$^{R/+}$, *Lgr5*$^{EGFP\text{-}IRES\text{-}CreERT2/+}$;*Rosa26*$^{R/+}$, and *Lgr5*$^{EGFP\text{-}IRES\text{-}CreERT2/+}$;*Rosa26*$^{+/+}$ mice were on the *C57BL6/J* background and were not injected with tamoxifen when used in experiments that did not involve lineage tracing.

Etoposide Treatment. The etoposide (NDC: 63323-104-50) dose that resulted in the death of fed but not fasted mice was determined for each strain and at each institution. Mice were allowed to feed ad libitum or were fasted for 24 h, followed by tail vein injection of etoposide. Experiments performed at Washington University School of Medicine used final doses of: 100 mg/kg for wild-type, *Bmi1*$^{CreERT/+}$;*Rosa26*$^{R/+}$ and *HopX*$^{CreERT/+}$;*Rosa26*$^{R/+}$ mice, and 80 mg/kg for *Lgr5*$^{EGFP\text{-}IRES\text{-}CreERT2/+}$;*Rosa26*$^{R/+}$ and *Lgr5*$^{EGFP\text{-}IRES\text{-}CreERT2/+}$ mice. Experiments performed at the MD Anderson Cancer Center, Houston used final doses of: 100 mg/kg for *Bmi1*$^{CreERT/+}$;*Rosa26*$^{R/+}$ mice and 110 mg/kg for *Lgr5*$^{EGFP\text{-}IRES\text{-}CreERT2/+}$;*Rosa26*$^{R/+}$ and *Lgr5*$^{EGFP\text{-}IRES\text{-}CreERT2/+}$ mice. After etoposide injection, moistened food pellets were placed at the bottom of all cages. Survival was monitored daily for 2 wk postinjection, unless otherwise noted. Mice and food were weighed daily.

Statistical Analysis. The statistical analyses used in this study are described in each figure legend.

ACKNOWLEDGMENTS. We thank Hiroyuki Mioyshi and Sofia Origanti for technical support and advice throughout the course of the study; Erin Smith and Lynne Collins for technical assistance in harvesting organs; all members of both the H.P.-W. and D.P.-W. laboratories and the T.S.S. laboratory for their input throughout the course of this study; and the Genome Technology Access Center at Washington University for help with genomic analysis. This study was supported in part by Grant P50 CA94056 to the Washington University-MD Anderson Cancer Center Inter-institutional Molecular Imaging Center; Grant P30 NS057105 to Washington University; Department of Defense Prostate Cancer Research Program Training Award Grant PC101951 (to K.L.T.); NIH National Institute of General Medical Sciences (NIGMS) Grant T32GM007200 (to A.J.L.); and NIH National Institute of Biomedical Imaging and Bioengineering (NIBIB) Grant T32EB018266 (to A.J.L.). The Genome Technology Access Center is partially supported by National Cancer Institute Cancer Center Support Grant P30 CA91842 to the Siteman Cancer Center and by Institute for Clinical and Translational Science/Clinical and

Translational Science Award UL1RR024992 from the National Center for Research Resources, a component of the National Institutes of Health, and National Institutes of Health Roadmap for Medical Research. H.P.-W. is a Research Professor of the American Cancer Society.

1. Bloechl-Daum B, Deuson RR, Mavros P, Hansen M, Herrstedt J (2006) Delayed nausea and vomiting continue to reduce patients' quality of life after highly and moderately emetogenic chemotherapy despite antiemetic treatment. *J Clin Oncol* 24(27): 4472–4478.
2. Chen Y, Jungsuwadee P, Vore M, Butterfield DA, St Clair DK (2007) Collateral damage in cancer chemotherapy: Oxidative stress in nontargeted tissues. *Mol Interv* 7(3): 147–156.
3. Farrell C, Brearley SG, Pilling M, Molassiotis A (2013) The impact of chemotherapy-related nausea on patients' nutritional status, psychological distress and quality of life. *Support Care Cancer* 21(1):59–66.
4. Raffaghello L, et al. (2008) Starvation-dependent differential stress resistance protects normal but not cancer cells against high-dose chemotherapy. *Proc Natl Acad Sci USA* 105(24):8215–8220.
5. Lee C, et al. (2012) Fasting cycles retard growth of tumors and sensitize a range of cancer cell types to chemotherapy. *Sci Transl Med* 4(124):124ra27.
6. Brandhorst S, Wei M, Hwang S, Morgan TE, Longo VD (2013) Short-term calorie and protein restriction provide partial protection from chemotoxicity but do not delay glioma progression. *Exp Gerontol* 48(10):1120–1128.
7. Shi Y, et al. (2012) Starvation-induced activation of ATM/Chk2/p53 signaling sensitizes cancer cells to cisplatin. *BMC Cancer* 12:571.
8. Safdie F, et al. (2012) Fasting enhances the response of glioma to chemo- and radiotherapy. *PLoS One* 7(9):e44603.
9. Boussios S, Pentheroudakis G, Katsanos K, Pavlidis N (2012) Systemic treatment-induced gastrointestinal toxicity: Incidence, clinical presentation and management. *Ann Gastroenterol* 25(2):106–118.
10. Hauer-Jensen M, Denham JW, Andreyev HJ (2014) Radiation enteropathy—pathogenesis, treatment and prevention. *Nat Rev Gastroenterol Hepatol* 11(8):470–479.
11. Rodier F, et al. (2009) Persistent DNA damage signalling triggers senescence-associated inflammatory cytokine secretion. *Nat Cell Biol* 11(8):973–979.
12. Coppe JP, et al. (2008) A role for fibroblasts in mediating the effects of tobacco-induced epithelial cell growth and invasion. *Mol Cancer Res* 6(7):1085–1098.
13. Pazolli E, et al. (2009) Senescent stromal-derived osteopontin promotes preneoplastic cell growth. *Cancer Res* 69(3):1230–1239.
14. Lee G, et al. (2011) Contributions made by CDC25 phosphatases to proliferation of intestinal epithelial stem and progenitor cells. *PLoS One* 6(1):e15561.
15. Sangiorgi E, Capecchi MR (2008) Bmi1 is expressed in vivo in intestinal stem cells. *Nat Genet* 40(7):915–920.
16. Yan KS, et al. (2012) The intestinal stem cell markers Bmi1 and Lgr5 identify two functionally distinct populations. *Proc Natl Acad Sci USA* 109(2):466–471.
17. Metcalfe C, Kljavin NM, Ybarra R, de Sauvage FJ (2014) Lgr5+ stem cells are indispensable for radiation-induced intestinal regeneration. *Cell Stem Cell* 14(2): 149–159.
18. Montgomery RK, et al. (2011) Mouse telomerase reverse transcriptase (mTert) expression marks slowly cycling intestinal stem cells. *Proc Natl Acad Sci USA* 108(1): 179–184.
19. Miyoshi H, Stappenbeck TS (2013) In vitro expansion and genetic modification of gastrointestinal stem cells in spheroid culture. *Nat Protoc* 8(12):2471–2482.
20. Miyoshi H, Ajima R, Luo CT, Yamaguchi TP, Stappenbeck TS (2012) Wnt5a potentiates TGF-β signaling to promote colonic crypt regeneration after tissue injury. *Science* 338(6103):108–113.
21. VanDussen KL, et al. (2015) Development of an enhanced human gastrointestinal epithelial culture system to facilitate patient-based assays. *Gut* 64(6):911–920.
22. Patel KK, et al. (2013) Autophagy proteins control goblet cell function by potentiating reactive oxygen species production. *EMBO J* 32(24):3130–3144.
23. Sato T, et al. (2009) Single Lgr5 stem cells build crypt-villus structures in vitro without a mesenchymal niche. *Nature* 459(7244):262–265.
24. Barker N (2014) Adult intestinal stem cells: Critical drivers of epithelial homeostasis and regeneration. *Nat Rev Mol Cell Biol* 15(1):19–33.
25. Potten CS, Owen G, Booth D (2002) Intestinal stem cells protect their genome by selective segregation of template DNA strands. *J Cell Sci* 115(Pt 11):2381–2388.
26. Barker N, et al. (2007) Identification of stem cells in small intestine and colon by marker gene Lgr5. *Nature* 449(7165):1003–1007.
27. Takeda N, et al. (2011) Interconversion between intestinal stem cell populations in distinct niches. *Science* 334(6061):1420–1424.
28. Tian H, et al. (2011) A reserve stem cell population in small intestine renders Lgr5-positive cells dispensable. *Nature* 478(7368):255–259.
29. Hua G, et al. (2012) Crypt base columnar stem cells in small intestines of mice are radioresistant. *Gastroenterology* 143(5):1266–1276.
30. Liu J, Kim J, Oberdoerffer P (2013) Metabolic modulation of chromatin: Implications for DNA repair and genomic integrity. *Front Genet* 4:182.
31. Sahm F, et al. (2013) The endogenous tryptophan metabolite and NAD+ precursor quinolinic acid confers resistance of gliomas to oxidative stress. *Cancer Res* 73(11): 3225–3234.
32. Kalaany NY, Sabatini DM (2009) Tumours with PI3K activation are resistant to dietary restriction. *Nature* 458(7239):725–731.
33. Safdie FM, et al. (2009) Fasting and cancer treatment in humans: A case series report. *Aging (Albany, NY)* 1(12):988–1007.
34. Levine ME, et al. (2014) Low protein intake is associated with a major reduction in IGF-1, cancer, and overall mortality in the 65 and younger but not older population. *Cell Metab* 19(3):407–417.
35. Committee on Care and Use of Laboratory Animals (1996) *Guide for the Care and Use of Laboratory Animals* (National Institutes of Health, Bethesda, MD), DHHS Publ No (NIH) 85-23.
36. Soriano P (1999) Generalized lacZ expression with the ROSA26 Cre reporter strain. *Nat Genet* 21(1):70–71.
37. Allen ND, et al. (1988) Transgenes as probes for active chromosomal domains in mouse development. *Nature* 333(6176):852–855.
38. Seinfeld JH, Pandis SN (2006) *Atmospheric Chemistry and Physics: From Air Pollution to Climate Change* (J. Wiley, Hoboken, NJ), 2nd Ed, p xxviii.
39. Guo J, Longshore S, Nair R, Warner BW (2009) Retinoblastoma protein (pRb), but not p107 or p130, is required for maintenance of enterocyte quiescence and differentiation in small intestine. *J Biol Chem* 284(1):134–140.
40. Huang W, Sherman BT, Lempicki RA (2009) Systematic and integrative analysis of large gene lists using DAVID bioinformatics resources. *Nat Protoc* 4(1):44–57.
41. Huang da W, et al. (2009) Extracting biological meaning from large gene lists with DAVID. *Curr Protoc Bioinformatics* Chapter 13:Unit 13.11.